Geologie en Mijnbouw **70**: 175–185, 1991.

Mass transfer in a porous medium by thermally driven fluid convection: a numerical model and its application to the Travis Peak Formation, East Texas

J. Gerretsen[1], W.H. Breeuwsma, H. de Boorder & C.J. Spiers
Institute of Earth Sciences, University of Utrecht, P.O. Box 80.021, 3508 TA Utrecht, The Netherlands
[1] Now at TNO, Centre for Technical Ceramics, P.O. Box 595, 5600 AN Eindhoven, The Netherlands

Received 15 November 1990; accepted in revised form 20 December 1990

Key words: mass transfer, porous medium, fluid convection, numerical model, Travis Peak Formation

Abstract

The diagenetic change of porosity by long range solution-precipitation mass transfer in a freely convecting porous medium is investigated by numerical modelling. From the conservation of mass and energy, assuming Darcian flow and local chemical equilibrium, making the Boussinesque approximation and neglecting deformation effects, a set of dimensionless partial differential equations is derived. These are then transformed into a set of algebraic equations, using a central finite difference method. Solutions were obtained using an implicit Gauss-Seidel relaxation method as well as an explicit method employing direct matrix inversion plus time stepping. The coupling between fluid flow behaviour (determined by the Rayleigh number) and local mass balance is established through a linear relation between the relative change in permeability and relative change in porosity. The results obtained for steady state convection omitting solute transport effects are in good agreement with numerical and laboratory scale experiments reported elsewhere. When solution-phase transport is permitted the reservoir porosity shows an exponential change with time at rates twice those predicted using a simpler analytical approximation.

The numerical model is used to evaluate the development of porosity in the Travis Peak Formation of East texas. This formation consists of well-sorted, fine-grained quartz arenites deposited in the Early Cretaceous. During the early stages of diagenesis, the average porosity decreased from 25% to 10% as a result of quartz cementation. Explanations based on an influx of warm meteoric fluids are questionable because of the large fluid-to-rock ratios required. However, taking into account geological constraints on heat flux, starting permeability and layer thickness, our numerical simulations show that long range solution transfer in a freely convecting closed system may well explain the rapid decrease of porosity observed in the Travis Peak Formation.

Introduction

Transport of dissolved inorganic material is an important process in the diagenetic modification of the storage capacity and fluid transmissivity of sedimentary rocks. Understanding this process is of great importance to exploration geologists in modelling the evolution of oil and gas reservoirs, in locating such reservoirs and in evaluating their capacity and productivity.

On the grain-scale, mass transfer may occur via diffusion, as is the case with the stress-induced

process of intergranular 'pressure solution'. On a larger scale, advection of fluids and solutes allows transport over long distances. Despite many studies of diagenetic processes in reservoir rocks (e.g. sandstones), the origin of cementing materials and the mechanism of transport remain a subject of considerable debate (Wood & Hewett 1982, Bethke 1985, Dutton & Land 1988). A point of particular difficulty is that the low solubility of minerals such as quartz requires large volumes of throughgoing meteoric water to acount for even minor amounts (a few percent) of precipitated cement (Dutton 1987). To illustrate this, a simple calculation shows that for a layer of rock with initial porosity of 30%, an area of 150 km^2 and 1 km thickness, 10^8 km^3 of water at upper crustal pressure and temperature would be required to reduce the porosity by about half through precipitation of all quartz in solution. This amount of fluid corresponds to a single layer of water approximately 200 m thickness covering the entire Earth. On the basis of such calculations, one cannot discard single pass fluid flow as a possible explanation for transport of cement materials. However, intra-formational, thermally driven (free) convection does offer an attractive alternative.

Given a pore fluid which expands with increasing temperature, stratification of the fluid will be stable when temperature decreases with depth. In this case, the colder and hence denser fluid is covered by warmer and less dense fluid. In the Earth, the temperature generally increases with depth. Such a thermal gradient may, in principle, induce fluid convection. However, when the buoyancy force arising from such a gradient is not large enough to overcome viscous drag in the fluid, and when lateral density perturbations cannot be maintained due to rapid heat transport, the increase in temperature with depth does not necessarily lead to convective motion. The criterion of convective instability is based on the Rayleigh number $R_a = \varkappa g \alpha \varrho_w C_w H \Delta T / \lambda \nu$, where $\varkappa$ is the permeability of the reservoir rock, g is the acceleration due to gravity, α is the thermal expansion coefficient of the fluid, ϱ_w is the fluid density, C_w is the heat capacity of the fluid, H is the thickness of the porous layer, ΔT is the temperature difference across that layer, λ is the effective thermal conductivity of the fluid-filled porous medium, and ν is the kinematic viscosity of the fluid. Instability analysis shows that when Boussinesque approximations are applicable (i.e. assuming that the effect of temperature on density is negligible except in the equation of motion, and taking constant viscosity), the critical value of the Rayleigh number corresponding to the onset of convection is $4\pi^2$.

It is commonly argued that convective fluid flow can only be achieved under a range of special conditions, for example large temperature differences in combination with high permeability and low viscosity (Norris & Henley 1976, Knapp & Knight 1977, Etheridge et al. 1983, Etheridge et al. 1984). This is a valid argument for a horizontal porous layer saturated with a fluid having constant values of ν, C_w, and λ. However, it might not hold in many geological cases. Firstly, the effect of temperature and pressure on the properties of the fluid is significant and must be taken into account. For example, under a temperature gradient of 40° C/km the critical Rayleigh number, as defined by Straus & Schubert (1977), decreases by a factor of 2 at a depth of 500 m with respect to the surface value. Secondly, lithological boundaries rarely coincide with surfaces of constant gravitational potential (Wood & Hewett 1982, 1984). Under these circumstances, the concept of a critical Rayleigh number no longer applies. Instead, the fluid motion occurs irrespective of the magnitude of the thermal gradient or rock permeability since isotherms are inclined with respect to the local geoid and lateral density gradients are maintained in the fluid (Wood & Hewett 1982).

On the basis of the above arguments, and assuming chemical equilibrium and negligible diffusional transport, Wood & Hewett (1982, 1984) derived an analytical approximation that predicts that intraformational transport of material by convection may be substantial. For densifying regions, they found an exponential decay of porosity with time. The relaxation time required for significant changes in porosity to occur was found to be around ten million years taking typical values for fluid and host rock properties, an average fluid flow of 1 m/yr, and assuming a temperature gradient of only 25° C/

km. On the basis of these approximations, Wood & Hewett (1982, 1984) concluded that in many geological cases eddy currents will be present and large scale mass transfer can account for a significant portion of the porosity change observed in reservoir rocks. Convective transport thus appears to offer a viable alternative to single pass fluid motion, not only under extreme conditions but in most porous media and especially in those cases where lateral density differences occur in the fluid.

In the present paper, the basic equations governing heat and mass transfer have been implemented in a two dimensional numerical model for convection in a porous medium characterized by a Rayleigh number which effectively exceeds the critical number. This describes the evolution of porosity and permeability in an initially homogeneous porous reservoir as a result of dissolution, transport and precipitation of the host material occurring via thermally driven (free) internal convection of the pore fluid phase. The numerical model is used to gain insight into the controversial question of porosity evolution in the cemented sandstones of the Travis Peak Formation, Texas (Dutton 1987, Dutton & Land 1988).

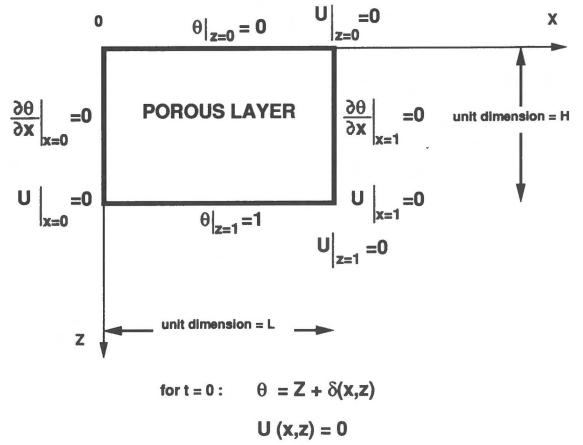

Fig. 1. Model geometry.

Mathematical model

Consider a horizontal layer with homogeneous thickness (H) and uniform starting permeability ($\varkappa_0$), temperature (T_0) and porosity (φ_0). The horizontal dimension (L) of the layer is much larger than the thickness (H) and convection is assumed to be two dimensional, i.e. fluid movement is constrained to the vertical plane (x, z; with z positive upwards). The porous body is saturated with a single phase fluid with constant kinematic viscosity, heat capacity and conductivity. Furthermore, it is assumed that the imposed temperature difference (ΔT) between the top and the bottom of the layer is constant and that no lateral heat exchange occurs at the vertical boundaries at x = 0 and x = L. The geometry of the layer is illustrated in Fig. 1. The porous rock is assumed to consist of only one mineral (density ϱ_s, heat capacity C_s) with a temperature and pressure dependent solubility in water. Solid and solute are assumed to remain in ideal chemical equilibrium at all points, and dissolution and precipitation occur instantaneously. Mechanical mixing and dispersion are neglected. Mechanical compaction and pressure solution are not explicitly accounted for in our mathematical model but are crudely accounted for in some of our simulations.

Free convection

Clearly, if the above layer is heated from below, an unstable situation will exist and the fluid can be set into convective motion with a velocity field defined by the vector **u**. Making the Boussinesque approximation and assuming $\varrho_s C_s \approx \varrho_w C_w$, the laws of mass and energy conservation (equations 1, 2) plus Darcy's law for fluid flow (equation 3) are written:

$$\nabla \cdot \mathbf{u} = 0 \tag{1}$$

$$\frac{\partial T}{\partial t} = \frac{\lambda}{\varrho_w C_w} \nabla^2 T - \mathbf{u}.\nabla T \tag{2}$$

$$\mathbf{u} = -\frac{\varkappa}{\mu}(\nabla P - \varrho_w \mathbf{g}) \tag{3}$$

Equations (1), (2) and (3) together describe the coupled processes of fluid flow and heat transport in the system. Here t denotes time and P is the

pressure in the fluid. Henceforth, expressing all quantities in dimensionless terms equations (1)–(3) can now be combined to yield the following set of equations:

$$\omega = R_a \frac{\partial \theta}{\partial x} \tag{4}$$

$$\nabla^2 \psi = \omega \tag{5}$$

$$V = \delta(\psi, \theta) \tag{6}$$

$$\frac{\partial \theta}{\partial t} = \nabla \theta - V \tag{7}$$

where ψ is the streamfunction defined such that the fluid velocity is given by $\mathbf{u} = (-\partial\psi/\partial z, \partial\psi/\partial x)$, ω is the fluid vorticity, defined through $\mathrm{rot}(\mathbf{u}) = \omega \mathbf{e}_y$ where $\mathbf{e}_y$ is the unit vector parallel to the y-direction, and θ is the dimensionless temperature $(T - T_0)/\Delta T$. The quantities ω and V are the 'source terms' and represent the generation of vorticity and temperature, respectively. The Jacobian operator δ is defined as:

$$\delta(\psi, \theta) = -\frac{\partial\psi}{\partial z}\frac{\partial\theta}{\partial x} + \frac{\partial\psi}{\partial x}\frac{\partial\theta}{\partial z} \tag{8}$$

In principle, it should be possible to solve equations (5) to (7) to obtain θ and ψ. However, in a system in which solute transport is allowed, porosity and permeability changes cause the value of R_a to change with time, and this must also be taken into account.

Solute transfer

From the mass balance for the solute and solid in a closed system in which solution phase transport occurs, it follows that the change in porosity with time is related to the change in the mass fraction of the solute (C) in the fluid phase. This relationship is expressed by the equations

$$\frac{\partial}{\partial t}(\varphi \varrho_w C) + \nabla \cdot (\varrho_w C \mathbf{u}) = \varphi D_{eff} \varrho_w \nabla^2 C + R \tag{9a}$$

$$\frac{\partial}{\partial t}((1 - \varphi)\varrho_s) = -R \tag{9b}$$

where D_{eff} is the effective diffusion coefficient of the solute in the fluid (including molecular diffusion and dispersion) and R is the rate of dissolution of quartz. Geological fluid flow rates ($|\mathbf{u}|$) are often of the order of 10^{-8} m/s (Wood & Hewett 1984). The relative contribution of the advective component of mass transport ($\mathbf{u} \cdot \nabla C/\varphi$) compared with diffusive transport ($D_{eff}\nabla^2 C$) is expressed by the Peclet number ($Pe = |\mathbf{u}| \cdot H/D_{eff}$). For a layer 100 m thick, Pe is of order of 1000 (Wood & Hewett 1982). This implies that the diffusional term in (9a) may be neglected. Because $\varphi\varrho_w C$ can be neglected in comparison to $(1 - \varphi)\varrho_s$, addition of (9a) and (9b) yields

$$\frac{\partial \varphi}{\partial t} = \frac{\varrho_w}{\varrho_s} \mathbf{u} \cdot \nabla C \tag{10}$$

where ϱ_s is assumed to be constant. Following Wood & Hewett (1984), the concentration gradient can be expressed in terms of the temperature and pressure dependencies of the solubility of the dissolved solid, represented by α_T and α_P, respectively. Thus

$$\frac{\partial \varphi}{\partial t} = \frac{\varrho_w}{\varrho_s} \mathbf{u} \cdot [\alpha_T \nabla T + \alpha_P \nabla P] \tag{11}$$

Rewriting this equation for variations along a streamline S we obtain

$$\frac{\partial \varphi}{\partial t} = \frac{\varrho_w}{\varrho_s} |\mathbf{u}| \left[\alpha_T \frac{dT}{dS} + \alpha_P \frac{dP}{dS}\right] \tag{12}$$

where $|\mathbf{u}|$ is the magnitude of the velocity along the streamline. In the numerical model $\alpha_P(dP/dS)$ has been neglected. Equation (12), taken together with equations (4) to (8), describes the coupled process of heat and mass transport in a freely convecting medium as well as the change in porosity due to dissolution, advective transport and precipitation. Coupling between equations (4) to (8) and (12) is established by the dependence of permeability on porosity. In general, there is no single expression for the relationship between the porosity of a rock and its permeability, and empirically derived relations are often assumed (Sharp & Domenico 1976). One such relation is the Kozeny-Carmen relationship, written

$$\varkappa = \frac{Ad^2\varphi^m}{(1-\varphi)^n} \tag{13}$$

where d is the average grain size and A is a constant representing sediment properties. For a wide range of rocks the exponents m and n fall in the range from 3 to 8 and 0 to 2, respectively (Sharp & Domenico 1976). Etheridge et al. (1984) suggested $m = 3$ and $n = 0$, with A in the range of 10^{-1} to 10^{-3}. In order to compare our model with the work of Wood & Hewett (1982, 1984), we follow them in choosing a simple linear relation between the permeability and the porosity change, namely

$$\frac{d\varkappa}{\varkappa} = \frac{d\varphi}{\varphi} \tag{14}$$

This provides the appropriate coupling between $\varkappa$ and φ, as a first approximation.

The removal and/or deposition of material as described by equation (12) when combined with expression (14) implies that porosity and permeability will increase when material is removed, and vice versa. This corresponds to the situation that only material directly in contact with the fluid channels is involved in the transfer process (Fig. 2b, d). As mentioned previously, porosity reduction by effects such as intergranular pressure solution (Fig. 2c) are neglected in the present analysis, though they may be significant in some cases.

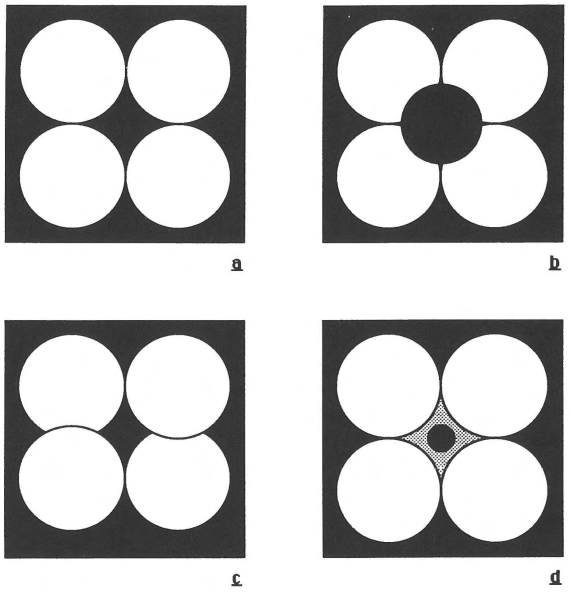

Fig. 2. Porosity development: a) starting material, b) porosity increase as a result of removal of material from the pore walls, c) porosity reduction as a result of removal of material from the grain boundaries and subsequent reduction of grain distance, d) reduction of the porosity by deposition of material on the wall of the pores.

Finite difference formulation

In order to numerically solve expressions (4) to (8), (12) and (14), the corresponding partial differential equations (p.d.e.'s) were discretized into a set of algebraic equations using the central finite difference method. These were solved at the nodes of a rectangular mesh of $N \times M$ grid lines (i, j) representing the reservoir layer. In our numerical approach, the following methods were employed:

(i) An implicit method employing Gauss-Seidel relaxation plus Liebmann's over-relaxation technique (Press et al. 1987). This method gives a slow but stable convergence to a solution. It was used to calculate steady state convection without mass transport, thereby allowing the validity of our approach to be directly tested against the work of Elder (1966, 1967a and b). In this approach the two Poisson-type p.d.e.'s (5) and (7) are solved stepwise, taking $\partial\varphi/\partial t = 0$.

(ii) An explicit method including direct matrix inversion by Gauss-Jordan elimination and back substitution (Press et al. 1987). In this case, the available computer memory limited the maximum grid size to 41×41 elements.

As mentioned above, the first method was used to model steady state convection only. The evolution of the reservoir with time, as a result of coupled convection and mass transport, was modelled using the second solution method plus a simple time stepping routine. Since all material properties (except solid solubility and ϱ_w) are taken to be independent of P and T, the matrix inversion step has to performed only once. Changes associated with each consecutive time-step can then be calculated by a simple matrix multiplication of the type $x = A^{-1}b$, with $Ax = b$ representing the set of

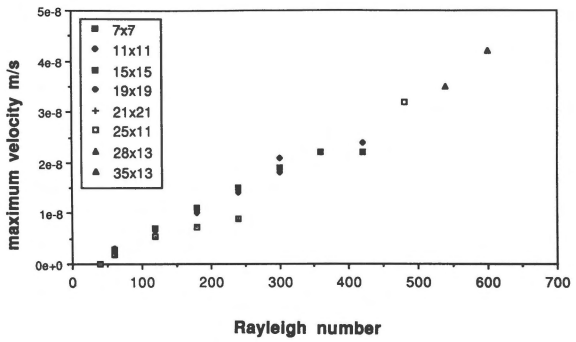

Fig. 3. Diagram showing the onset of numerical instability with increasing Rayleigh number for a range of grid dimensions.

algebraic equations derived from the discretised p.d.e.'s. Numerical stability was achieved using the constraint that, for advection-dominated transport, the time increment for each step should be less than the time required for a particle to traverse the mesh spacing.

Boundary and initial conditions

In our two-dimensional reservoir model, the following boundary conditions (b.c.) were imposed:

(i) The temperatures at the top and bottom are fixed (Dirichlet type b.c.) and remain constant with time such that $\theta|_{z=0} = 0$ and $\theta|_{z=1} = 1$.

(ii) Heat transfer at the vertical boundaries is assumed to be negligible (Neumann type b.c.), so that at $x = 0$ and $x = L/H$ no lateral temperature gradients exist. Thus $\partial\theta/\partial x|_{x=0,L/H} = 0$.

(iii) At $t = 0$, it is assumed that there is no flow and that the transfer of heat occurs only by conduction. Initially $\psi = 0$. The temperature increases linearly with depth according to $\theta(z) = z$. In order to prevent computational round-off errors from influencing the fluid flow pattern, the temperature field at $t = 0$ is perturbed randomly using the relation $\theta(z) = z + \delta(x,z)$, with perturbations $\delta(x,z)$ of the order of 10^{-3}.

(iv) Fluid flow is contained within the grid, so that ψ is zero at all boundaries.

Rayleigh number and numerical stability

A number of simulations for steady state convective heat transfer *without* solute transport were performed for a wide range of conditions defined in terms of the Rayleigh number in order to check the stability of the model. With increasing Rayleigh number, fluid flow becomes concentrated in narrow boundary layers thus introducing steep gradients in the temperature and velocity fields. If these become too steep, numerical instability results. The maximum Rayleigh number for numerically stable calculations is directly related to the number of grid points, the aspect ratio of the grid, and the round-off errors in the finite difference approximation. When solving the set of discretized finite difference equations by direct matrix inversion, for the case of fluid flow with zero mass transport, numerical stability could be obtained for larger values of the Rayleigh number. The numerical stability obtained by this model as function of grid size and Rayleigh number is illustrated in Fig. 3, in terms of maximum velocity.

Results

The results of our numerical experiments for zero mass (solute) transport are in good agreement with the results of Elder (1967a). Below a Rayleigh number of $4\pi^2$ no convection occurs and the so-called Nusselt number (a dimensionless measure of the heat transfer coefficient; measures the efficiency of the heat transfer process in terms of the proportion of advective and conductive heat transport) is 1. The dependence of the calculated Nusselt number upon the Rayleigh number is similar to that seen in the laboratory and numerical experiments of Elder (1967b).

The numerical experiments carried out allowing for mass transport show that steady state convection is reached long before any significant material transport has taken place (see Fig. 4a). This implies that initial conditions will not have a significant influence on the final results concerning the evolution of porosity. An example of typical results obtained in runs allowing mass transport is illustrated

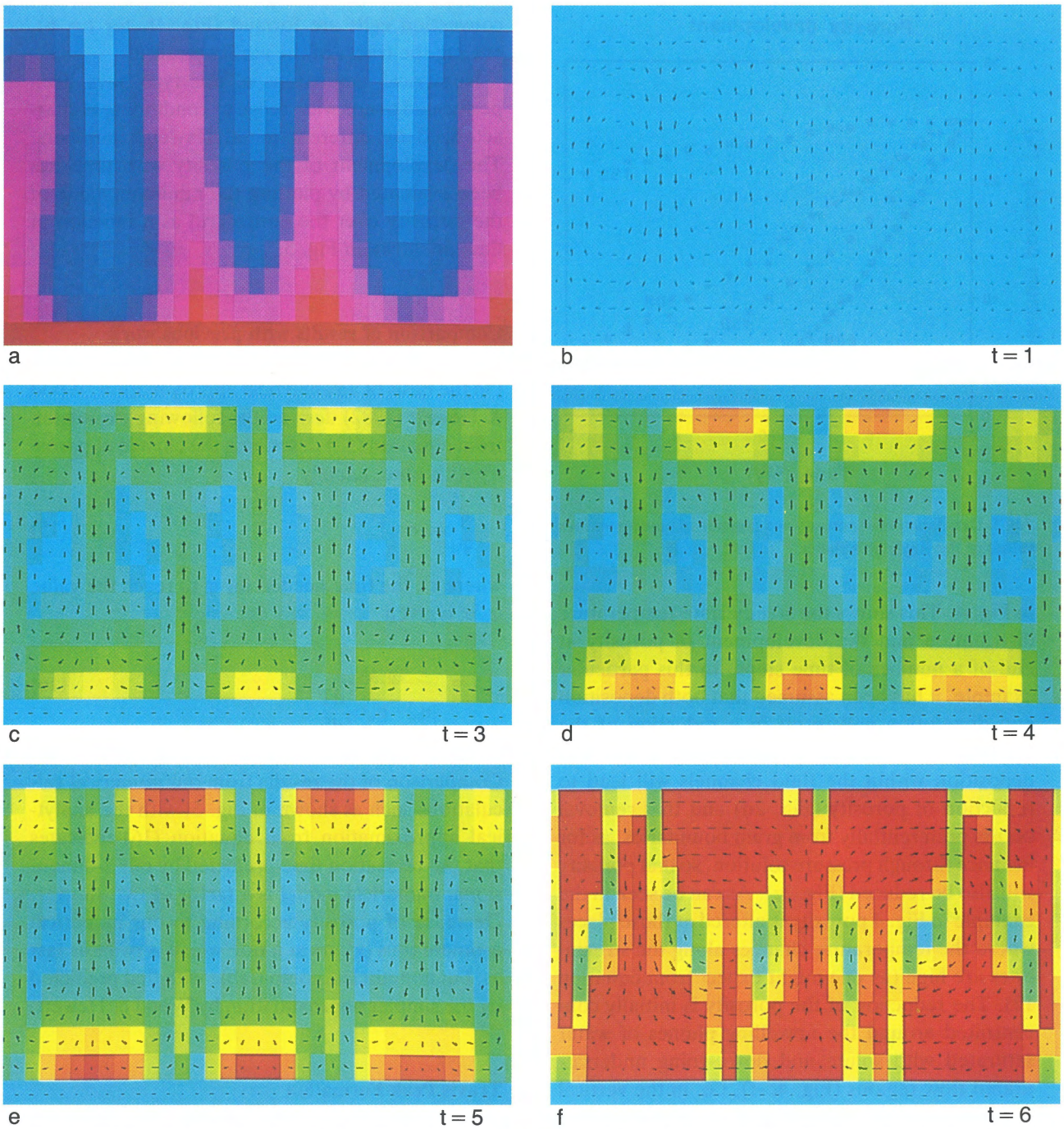

Fig. 4. Various stages of development of porosity reduction by intra-formational, thermally driven free convection (black arrows). a) Steady state temperature distribution achieved before significant mass transfer has taken place (light blue corresponds with $\theta = 0$, dark red with $\theta = 1$). b–f) Evolution of porosity and convective flow pattern with time typically obtained for Rayleigh numbers in the range 150–600 (green is 25% and brown less than 5% porosity). The time steps (t) between frames can be viewed as equivalent to periods of the order of 1–10 My.

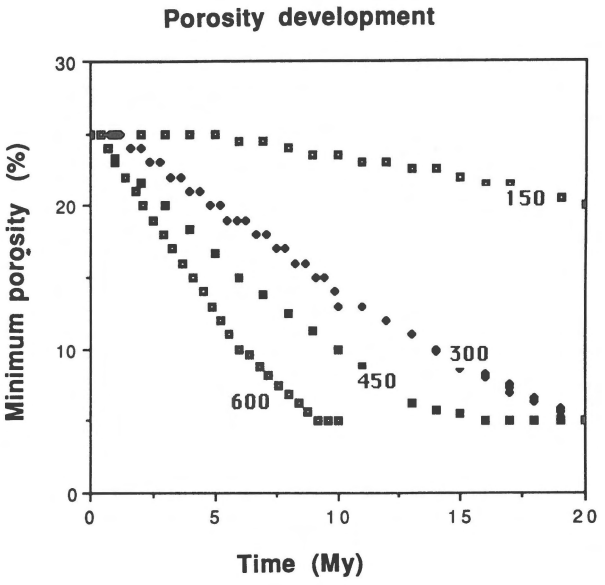

Fig. 5. Development of porosity as a function of time for various values of the Rayleigh number.

in Fig. 4. This shows the steady state temperature distribution and the development of porosity at end of a number of time steps. In this particular example, it has been assumed that both deposition and dissolution will result in a reduction of the porosity. This corresponds to the situation that deposition within the fluid channels will lead to reduction of porosity (Fig. 2d) and that removal occurs preferentially from grain boundaries, as for instance through pressure solution, so that porosity will also be reduced (Fig. 2c). As can be seen in the example in Fig. 4 porosity is altered at those places where the temperature changes along the streamlines are high (as one might expect from equation 12). The reduction of the porosity is initially concentrated around the upwelling plumes of water saturated with solute and down-going undersaturated flow regions (Fig. 4c–f), i.e. in the vertical limbs of convection cells. This leads to a strong lateral variation in porosity. With time, the fluid motion becomes increasingly concentrated in narrow zones surrounding islands of relatively little fluid motion with essentially unaltered porosity and small lateral temperature differences. After extensive porosity reduction has taken place, the initial flow pattern becomes unstable and larger convection cells are formed (Fig. 4f, for t = 6), erasing the traces of the earlier pattern.

Numerical simulations of this type have been performed over a wide range of conditions, as characterized by different initial Rayleigh numbers. The development of the porosity with time has been evaluated by plotting the minimum value of the porosity over the entire grid as a function of time as shown in Fig. 5.

Comparison of results with previous work

On the basis of an analytical approximation, Wood & Hewett (1982) derived the following expression from equation (12) describing the change of porosity with time, namely

$$\frac{\varphi}{\varphi_0} = e^{-\frac{t}{\tau}} \tag{15}$$

where τ, the time needed for φ to reach the value φ_0/e, is given

$$\tau = \frac{\varphi_0 \cdot \varrho_s}{|\mathbf{u}_0| \cdot \varrho_w \alpha_T \frac{dT}{dS}} \tag{16}$$

Comparison of the results from our numerical calculations such as shown in Fig. 5, with the analytical approximation from equation (16) indicates that the relaxation time predicted by our 2-dimensional numerical model is a factor of two shorter. Decrease of porosity according to our numerical estimate thus occurs at a rate which is twice as fast as, but nonetheless comparable with that predicted by the simpler approximation by Wood & Hewett.

Travis Peak Formation

The numerical model presented here has been used to evaluate the porosity evolution in the Travis Peak Formation of East Texas. This particular formation has been extensively studied and documented (Dutton 1987, Dutton & Land 1988, Laubach 1988). The formation consists of clean, well-sorted, fine-grained quartz arenites deposited in

the Early Cretaceous. The sandstone formation has been modified substantially during burial diagenesis. During the early stages of diagenesis the average porosity decreased from 25 to 10% as a result of quartz cementation. Although the overall burial history is complex, quartz cementation is inferred to have occurred in a well defined time span, i.e. after the precipitation of illite and the formation of dolomite, and preceding albitization of plagioclase and dissolution of orthoclase (Fig. 6). On this basis, quartz cementation can be regarded as a single event, concerning only one mineral in contact with a fluid, and does not appear to be influenced by other diagenetic processes. Cementation of the Travis Peak Formation can therefore be regarded as an excellent case for comparison with our model.

The total thickness of the Travis Peak Formation in which closed-cell convection could have occurred has been estimated from regional structural cross sections by Wood & Gueverra (1981) to be 1100 m. In addition, the temperature gradient during the burial history has been estimated to lie between 38° C/km (present day value) and 44° C/km (Dutton & Land 1988). The average value of pre-cement porosity was probably around 25% (Dutton 1987). Reduction of this value down to 7.5% (just below the top) or 3–5% (in the lower part of the formation), occurred by precipitation of quartz cement within a time span of 10 to 15 million years. The conditions as described here for the Travis Peak Formation correspond to a Rayleigh number of $150\varkappa$, where $\varkappa$ is the permeability (in Darcy) of the reservoir material prior to the onset of cementation ($R_a = 150$ for $\varkappa = 1$ Darcy $\sim 10^{-12}\,m^2$).

The actual permeability level prior to cementation is not known. However, using measured permeability versus cement volume data obtained from partially cemented rock samples (Dutton 1987), and extrapolating to zero cement content should give an indication of the order of magnitude of the pre-cementation permeability. Due to the wide spread in Dutton's (1987) data, such an extrapolation yields permeability values ranging from 10 Darcy or more down to less than 0.001 Darcy, with an average close to 0.5 Darcy. This extrapolation

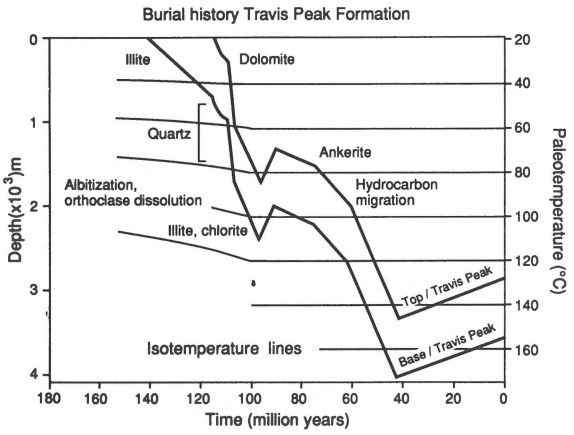

Fig. 6. Diagenetic burial history of the Travis Peak Formation showing the quartz cementation event after illite precipitation and dolomitization and prior to albitization and orthoclase dissolution (after Dutton, 1987).

does not take into account the effect of compaction due to dissolution and removal of framework grains. Therefore the starting permeability may have been as high as a few Darcy.

In order to apply our model to the Travis Peak Formation we ideally need a more realistic relation between the permeability and porosity of the formation than that expressed by equation (14). Dutton (1987) has extensively investigated the permeability of the Travis Peak Formation versus its porosity and cement content (see also Dutton & Land 1988). However, in order to interpret her data adequately, a further analysis is required. The data published by Dutton (1987) show a wide spread in values for permeability, porosity and the quartz cement content as a function of depth and cannot be interpreted in terms of a single porosity reduction process. For instance, the correlation coefficient for the relationship between volume of quartz cement in matrix-free sandstone and the logarithm of unstressed permeability is less than -0.54. Dutton attributes the low correlation coefficient to the fact that the two measurements of permeability and porosity were not made on the same sample. Although this may contribute to a reduced correlation, we suspect that the variability in the data might well be due to the simultaneous contribution of more than one mechanism to the reduction of

the porosity. The permeability may be reduced by deposition of quartz cement in the pores but may also be reduced by intergranular mass removal as shown schematically in Fig. 2c. In general, the simultaneous operation of these two mechanisms in differing proportions will, for a given cement content, lead to a scatter in permeability values. Considering the fairly uniform grainsize of the sandstone, the spread in data cannot be explained by a variation in the permeability at the onset of diagenesis.

From the above considerations it follows that although a large data set is available one cannot, as yet, be conclusive about the operating mechanisms and their contribution and further analysis has to be done. As a first approximation for our numerical simulation of the development of the Travis peak Formation we have chosen for the simple linear relation between permeability and porosity as expressed by equation (14).

It will be clear from our numerical results, as represented in Fig. 5 that for Rayleigh number values appropriate for the evolution of the Travis Peak Formation, the porosity reduction could well have taken place within the time interval available (i.e., 10–15 my, Fig. 6). Our numerical simulation shows that, given the available geological constraints on heat flux and layer thickness, the porosity evolution in a freely convecting closed system may well explain the rapid decrease of porosity observed.

When taking into account the effect of T and P on the fluid properties as discussed by Straus & Schubert (1977), the critical Rayleigh number is predicted to decrease with depth and the fluid velocity will increase as a result of a reduction of the dissipation by processes such as internal friction and heat conduction. One might expect that this effect will shorten the relaxation time, thereby making the concept of internal mass transport by free convection even more plausible, both in general and with reference to the Travis Peak Formation. The same comment can be made for the effect of non-parallelism of geotherms with surfaces of constant gravitational potential. Although no attempts have been made to implement and evaluate the extent of this effect, it is has been reported (Dutton & Land 1988) that the Travis Peak Formation was deposited in a tectonically active region associated with crustal stretching and rifting of the Gulf of Mexico. It is therefore not unlikely that deformation might have led to inclination of the geotherm with reference to the geoid, thereby contributing to the fluid movement.

Acknowledgements

Helpful comments and suggestions by Dr. S.M. Hassanizadeh are highly appreciated.

References

Bethke, C.M. 1985 A numerical model of compaction-driven groundwater flow and heat transfer and its application to the paleohydrology of intercratonic sedimentary basins – J. Geophys. Res. 90: 6817–6828

Dutton, S.P. 1987 Diagenesis and burial history of the Lower Cretaceous Travis Peak Formation, East Texas – Bureau of Ecomonic Geology, Univ. Texas, Austin, Rep. Inv. 164: 58 pp

Dutton, S.P. & L.S. Land 1988 Cementation and burial history of a low-permeability quartz arenite, Lower Cretaceous Travis Peak Formation, East Texas – Geol. Soc. Am. Bull. 100: 1271–1282

Elder, J.W. 1966 Numerical experiments with free convection in a vertical slot – J. Fluid Mech. 24: 829–843

Elder, J.W. 1967a Steady free convection in a porous medium heated from below – J. Fluid Mech. 24: 29–48

Elder, J.W. 1967b Transient convection in a porous medium – J. Fluid Mech. 27: 609–623

Etheridge, M.A., V.J. Wall & R.H. Vernon 1983 The role of the fluid phase during regional metamorphism and deformation – J. Metam. Geol. 1: 205–226

Etheridge, M.A., V.J. Wall, S.F. Cox & R.H. Vernon 1984 High fluid pressures during regional metamorphism and deformation: implications for mass transport and deformation mechanisms – J. Geophys. Res. 89: 4344–4358

Knapp, R. & J.E. Knight 1977 Differential thermal expansion of pore fluids: fracture propagation and microearthquake production in hot pluton environments – J. Geophys. Res. 82: 2515–2522

Laubach, S.E. 1988 Subsurface fractures and their relationship to stress history in East Texas basin sandstone – Tectonophysics 156: 37–49

Norris. R.J. & R.W. Henley 1976 Dewatering of the metamorphic pile – Geology 4: 333–336

Press, W.H., B.P. Flannery, S.A. Teulosky & W.T. Vetterling 1987 Numerical Recipes – Cambridge Univ. Press: 818 pp

Sharp, J.M. & P.A. Domenico 1976 Energy transport in thick sequences of compacting sediments – Geol. Soc. Am. Bull. 87: 390–400

Straus, J.M. & G. Schubert 1977 Thermal convection of water in a porous medium: effect of temperature- and pressure-dependent thermodynamic and transport properties – J. Geophys. Res. 82: 325–333

Wood, D.H. & E.H. Gueverra 1981 Regional structural cross sections and general stratigraphy, East Texas Basin – Bureau of Economic Geology, Univ. Texas, Austin: 21 pp

Wood, J.R. & T.A. Hewett 1982 Fluid convection and mass transfer in porous sandstones – a theoretical model – Geochim. Cosmochim. Acta 46: 1707–1713

Wood, J.R. & T.A. Hewett 1984 Reservoir diagenesis and convective fluid flow – Am. Ass. Petrol. Bull. Mem. 37: 99–110